UDC 621.314 https://doi.org/10.20998/2074-272X.2022.6.06

B.V. Sai Thrinath, S. Prabhu, B. Meghya Nayak

Power quality improvement by using photovoltaic based shunt active harmonic filter with Z-source inverter converter

Introduction. *The major source of energy for a long time has been fossil fuels, however this has its drawbacks because of their scarcity, exhaustibility, and impossibility of reusing them. Presently, a shunt active harmonic filter-equipped two-stage solar photovoltaic system is showing off its performance shunt active harmonic filter. The global power system has been impacted by current harmonics during the most modern industrial revolution.* ***Novelty.*** *The proposed work is innovative, by adopting the hysteresis modulation mode with Z-source inverter to enhance the performance of the system. Furthermore, the shunt active harmonic filter also get assists in this system for better improvement in the quality of power.* ***Purpose.*** *By incorporating an impedance source inverter and a photovoltaic shunt active harmonic filter methods, harmonic issues are mitigated.* ***Methods.*** *Load compensation is one of the services that the shunt active harmonic filter offers, in addition to harmonic compensation, power factor correction, and many other functions. The current pulse width modulation voltage source inverter method is more expensive, requires two converters owing to its two-stage conversion, has significant switching losses, and has a low rate of the reaction. The new model, in which the voltage source inverter is substituted out for a Z-source inverter converter, has been developed in order to address the problems of the existing system.* ***Results.*** *Rather than using a hybrid of DC-DC and DC-AC converters, the suggested system uses a shunt active harmonic filter that is powered by a photovoltaic source using a Z-source inverter. Utilizing Z-source inverter helps to address the present issues with conventional configurations.* ***Practical value.*** *By using software MATLAB/Simulink, this photovoltaic shunt active harmonic filter technique is analyzed. Shunt active harmonic filter, which produces compensatory current from the reference current obtained as from main supply, is powered by the photovoltaic array.* References 18, table 2, figures 13.

Key words: **photovoltaic, shunt active harmonic filter, Z-source inverter, PI controller, pulse width modulation.**

Вступ*. Основним джерелом енергії довгий час були викопні види палива, проте це мало свої недоліки через їх дефіцит, вичерпність та неможливість їх повторного використання. В даний час двоступенева сонячна фотоелектрична система, обладнана активним шунтуючим фільтром гармонік, демонструє свої робочі характеристики шунтуючого активного фільтра гармонік. На глобальну енергетичну систему вплинули гармоніки струму під час найсучаснішої промислової революції.* ***Новизна****. Пропонована робота є інноваційною, оскільки вона використовує режим гістерезисної модуляції з інвертором Z-джерела для підвищення продуктивності системи. Крім того, шунтуючий активний фільтр гармонік також допомагає в цій системі для покращення якості електроенергії.* ***Мета****. Включення інвертора джерела імпедансу та методів активного фільтру гармонік із фотогальванічним шунтом знижує гармонійні проблеми.* ***Методи****. Компенсація навантаження – це одна з функцій, які шунтуючий активний фільтр гармонік пропонує на додаток до компенсації гармонік, корекції коефіцієнта потужності та багатьох інших функцій. Інверторний метод широтно-імпульсної модуляції струму дорожчий, вимагає двох перетворювачів через його двокаскадного перетворення, має значні втрати комутації і має низьку швидкість реакції. Нова модель, в якій інвертор джерела напруги замінює перетворювач інвертора Z-джерела, була розроблена для вирішення проблем існуючої системи.* ***Результати****. Замість використання гібрида перетворювачів постійного та змінного струму в запропонованій системі використовується активний шунтуючий фільтр гармонік, який живиться від фотоелектричного джерела з використанням інвертора Z-джерела. Використання інвертора з Z-джерелом допомагає вирішити проблеми з традиційними конфігураціями.* ***Практична цінність****. За допомогою програмного забезпечення MATLAB/Simulink аналізується метод активного фільтру гармонік фотоелектричного шунта. Шунтуючий активний фільтр придушення гармонік, який виробляє компенсаційний струм із опорного струму, отриманого від мережі, живиться від фотоелектричної батареї.* Бібл. 18, табл. 2, рис. 13.

Ключові слова: **фотовольтаїка, шунтуючий активний фільтр придушення гармонік, інвертор Z-джерела, ПІ-регулятор, широтно-імпульсна модуляція.**

Introduction. The main issues with a practical photovoltaic (PV) system include power loss owing to variations in operating circumstances, such as temperature or irradiance, the significant computing burden imposed by contemporary maximum power point tracking (MPPT) techniques, and optimizing the PV array output during abrupt weather patterns. The perturb and observation (P&O) strategy is chosen for the majority of PV systems [1].

In [2] investigates a solar control system simulation model that can be applied to PV power plants or the construction of solar inverters. This approach combines a DC-DC boost converter utilizing the MPPT methods conductivity, iterative, and P&O. In [3] Nowadays, one of the key elements influencing an economic growth is power quality. In order to meet consumer demand, utilities must supply more electricity as the population increases. The difficulties and worries that occur from the addition of solar power to the grid are examined in this research. In grid-connected solar systems, the shunt active power filter (SAPF) with PI controller is aimed at enhancing power quality. In [4] presently, among the most popular power electronics topology is Z-source inverters (ZSI). This article gives a brief introduction to the ZSI and examines its many topologies in depth, as well as the use of ZSI in the industrial applications. In [5] comprised of two control operations, the first of which uses a fuzzy logic controller to extract the maximum energy point from a PV panel's DC-DC converter. The main objective of this study, as stated in [6], is to decrease network power loss while simultaneously enhancing the bus voltage stability. This paper presents the modeling and simulation outcomes of a static compensator premised on a ZSI. In [7] when the decoupled double synchronous reference frame theory may be used to extract the magnificent of currents and prevent double frequency oscillations induced by introducing positive and negative-sequence currents into unbalanced, nonlinear loads. A three-level voltage source converter design is used for SAPF implementation and will provide compensating at the point of common coupling (PCC). Shunt active harmonic filter (SAHF) is employed in [8] to reduce the current harmonics. The process utilized to derive the reference current affects the filter's performance and precision. A three-phase SAHF, phase locked loop, and hysteresis are used in this study. The IGBT-based SAHF is activated by hysteresis switching [9].

In [10] resents a two stage ZSI for a PV single phase application. Here, ZSI includes an additional mode called the shoot through state, which allows it to function in a single stage, or even as a boost converter with voltage source inverter (VSI). ZSI outperforms BC+VSI in terms of downsides. A solar PV source is linked to an interactively three-phase SAPF in [11] through some kind of ZSI.

The proposed resolution aims to reduce the total harmonic distortion (THD) of the source current [12]. In a solar system that is linked to the grid, the harmonics caused by non-linear loads cannot be efficiently compensated by ordinary LC filters. The SAHF is presented due to its qualities and abilities for harmonic mitigation. The filter control system's primary focus is on producing reference source current, and this paper is used to reduce the harmonic currents [13].

In [14-18] power systems are using non-linear loads more and more frequently. This includes equipment like UPSs, inverters, converters, and others of a similar nature. These loads result in harmonics, which are quasi and distorted currents, in the source current. The P&O method is used to track the rated maximum characteristics of the PV module. The harmonic injection techniques are investigated and analyzed for grid connected system. The OPAL-RT-5600 is implemented under many circumstances by multi-variable filter associated with synchronous reference frame controller to reduce harmonics and to inject active power to the grid.

Modeling of PV & SAHF with VSI.

A) PV module. A PV system is made up of solar panels that use the photoelectric effect to transform solar light directly into electricity. Figure 1,*a* shows the equivalent circuit diagram for a solar cell, where R_s and R_{sh} stand for series and shunt resistance, respectively. The properties of *I-V* and *P-V* are shown in Fig. 1,*b*.

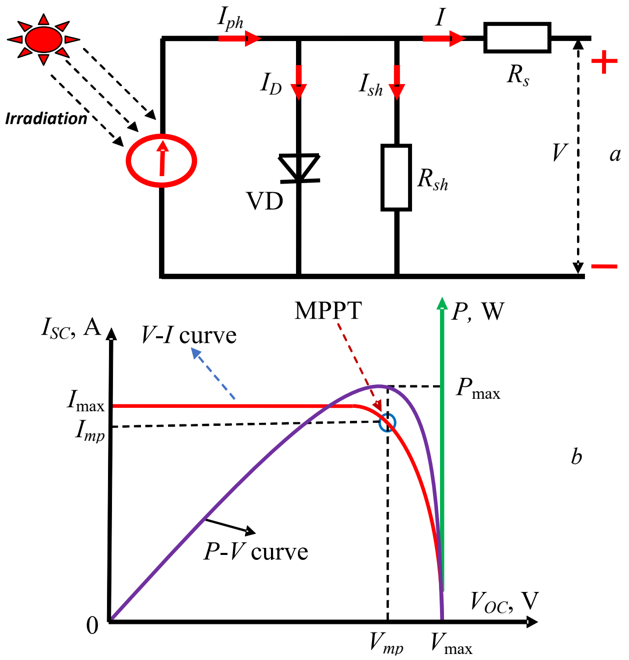

Fig. 1. *a* – simplified equivalent circuit diagram of PV cell; *b* – *I-V* and *P-V* characteristics of PV cell

According to the Shockley theory, the diode current is:

$$I_d = I_s\left[\exp\left(\frac{q\cdot V}{n\cdot K\cdot T}\right)-1\right], \quad (1)$$

where I_s is the transistor saturate current; q is the electron charge; V is the voltage; K is the Boltzmann constant; n is the ideal factor; T is the cell temperature.

Since the two boundary elements of a PV module, namely V_{oc} and I_{sc}, are found by first reducing V=0 to produce I_{sc} and afterwards V_{oc} by setting cell current I=0, equation (1) results in:

$$V_{oc} = \frac{n\cdot K\cdot T}{q}\cdot\ln\left(\frac{I}{I_0}\right). \quad (2)$$

The output of the PV cells changes with solar irradiation, hence the MPPT tracking algorithm is employed to make sure the PV system is operating as efficiently as possible. The formula d($V{\cdot}I$)/dt = 0 provides the maximum voltage level. Then,

$$V_{oc} = V_{oc} - \frac{K\cdot T}{q}\cdot\ln\left[\left(\frac{V_{mp}\cdot q}{n\cdot K\cdot T}\right)+1\right]. \quad (3)$$

Cell junction quality can be measured by the form factor, which is provided by:

$$FF = \left(\frac{V_{mp}\cdot I_{mp}}{V_{oc}\cdot I_{sc}}\right). \quad (4)$$

The quality is greater the closer the level of form factor is near unity. Furthermore, the following factors are used to determine the PV module's efficiency:

$$\%\eta = \left(\frac{FF\cdot V_{oc}\cdot I_{sc}}{P_{in}}\right). \quad (5)$$

B) Shunt active harmonic filter. SAPFs injected an equal but adverse harmonic compensation current to minimize current harmonics. The SAPF acts as a current source in this scenario, injecting the phase-shifted by 180° harmonic components produced by the loads. As a result, the active filter's impact wipes out harmonic current components present in the load current, keeping the source current continuous and in phase also with proper phase-to-neutral voltage. Any kind of load regarded as a harmonic source can be used in accordance with this concept. Additionally, the active power filter may correct the load power factor with the right control strategy. The active power filter and irregular load are viewed as the perfect resistor by the power distribution network in this way. Figure 2 displays the SAPF's compensating characteristic features.

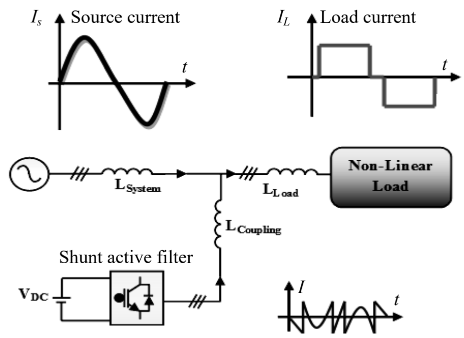

Fig. 2. Shunt active harmonic filter

A reference current is initially produced by the SAHF employing a PI controller. The advantage of this technique is that it eliminates the need for synchronizing with the phase voltage. The hysteresis controller design the switching pulse through pulse width modulation (PWM) from the reference current as well as the current needed to configure the DC link capacitor.

The voltage of the immediate supply is:

$$V_S(t) = V_{SM}\sin(\omega t). \qquad (6)$$

At PCC, nodal analysis provides the source current:

$$I_s(t) = I_L(t) - I_H(t). \qquad (7)$$

then $I_L(t)$ is indicated as:

$$I_L(t) = I_1\sin(\omega t + \Phi_1) + \sum_{h=0}^{\infty} I_h \sin(n\cdot\omega t + \Phi_h). \qquad (8)$$

The harmonics element is the second terminology used here. The load current and supply voltage may be used to compute the instantaneous value of the load demand.

Calculating the total power demand is as follows:

$$P_L(t) = I_L(t)\cdot V_S(t). \qquad (9)$$

As from load power, the true power may be calculated as follows:

$$P_f(t) = V_{SM}\cdot I_1\sin^2(\omega t)\cdot\cos\Phi_1 = V_S(t)\cdot I_S(t). \qquad (10)$$

Following compensating, the source current would be:

$$I_S(t) = \frac{P_f(t)}{V_S(t)} = I_1\cdot\cos\Phi_1\cdot\sin(\omega t) = I_{SM}\cdot\sin(\omega t). \qquad (11)$$

where I_{SM} is the maximum source current magnitude.

C) SAHF with VSI. The SAHF system, which is coupled in a parallel arrangement with a non linear load, is powered by a PV array system that is implemented with a P&O MPPT controller, as shown in Fig. 3.

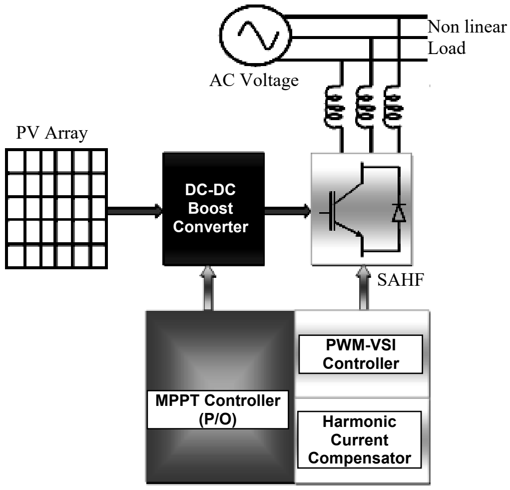

Fig. 3. SAHF with VSI

PWM-VSI controller is used to construct the SAHF. The switching pulse for VSI is produced using an adaptable hysteresis regulator. The reference current is extracted by the PI controller. To create switching pulses, the reference current that was extracted is then compared to the supply current. The source current's components are introduced by the nonlinear load. In order to diminish the harmonics present in the source current and make it sinusoidal and in phase with the input signal, the SAHF creates compensatory current that is the same size as the source current but also with a 180° phase shift. Sensing the baseline current taken from the power supply generates the compensatory current.

Proposed topology.

A) SAHF with impedance source inverter. In Fig. 4 by combining PV-based SAHF plus ZSI, the recommended method addresses issues with power quality. Researchers enhanced power quality in the prior method using PV-based SAHF with VSI. In this method, the maximum power is tracked by the P&O algorithm utilizing the MPPT methodology, a boost converter, a VSI, and other devices. The ZSI, SAHF, PV array, and other important building blocks are included in the recommended approach. We can reduce expenses, boost response rates, and just do deal with two-stage conversion thanks to this novel technique. Only one difference between the operation and the existing technique is the substitution of ZSI for BC+VSI.

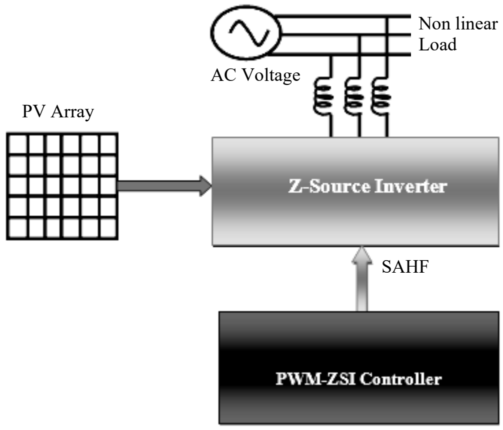

Fig. 4. SAHF with ZSI

Figure 5 illustrates the ZSI distinctive impedance network, which consists of 2 splitting inductors and 2 X-shaped capacitors. The three-phase ZSI bridge has nine switching states, as opposed to the normal VSI's eight. When the load connections are short circuited either via the bottom 3 switching devices or even the top 3 switching devices, accordingly, the ZSI has 6 original states when the DC link voltage is impressing across the three-phase loads and 2 zero states.

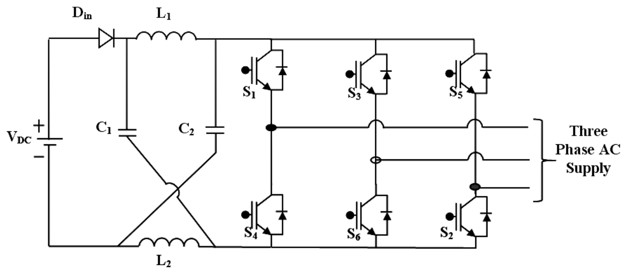

Fig. 5. Impedance source inverter

The Z-network is in charge of accelerating and monitoring the MPPT. The total power received by the inverters from the DC supply will determine the Shoot through switching frequency T_0/T (P&O technique). The MPPT tracking used in the conventional BC+VSI topology is the same as this. When combining it with ZSI, the switching frequency at MPPT uses the entire amount of electricity from the PV panel.

B) Operating modes. Depending on the inverter bridge's power switches, the ZSI can operate in one of three different ways, as seen below.

Mode 1. Null stator zero state. In this condition, an open circuit is analogous to an inverter bridge. Switches (S1, S3, S5) or (S2, S4, S6) are in the ON position in this condition.

Mode 2. Active stator non-shoot through state. Six states are currently operational. In the ON state are (S1, S3, S6), (S3, S5, S2), (S5, S1, S4), (S2, S4, S5), (S4, S6, S1), or (S6, S2, S3). As the load is shorted through either the upper or lower 3 switching devices, the inverter bridging is from one of 2 zero states. In this state, as illustrated in Fig. 6, the bridge can be thought of as an open-circuit (current source with really no current flowing.

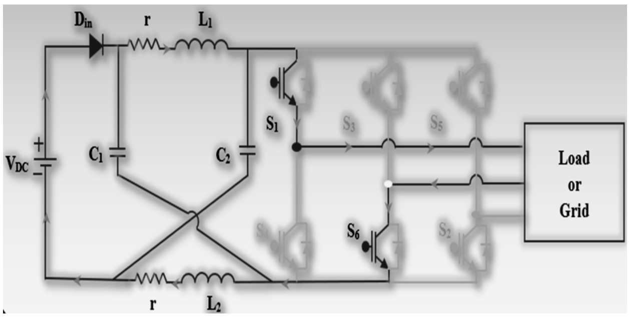

Fig. 6. Equivalent circuit of ZSI viewed from the DC link when the bridge is in an on-shoot through mode

Although there is no current flowing from the DC source to the load, the DC source's voltage may be seen between both the inductor as well as the capacitor. Switches on the identical leg of the 3 phase inverter are activated. It resembles a short circuit. S1 through S6 are in the ON position. One of the 7 shoot through (ST) modes is being used by the inverter bridge. The bridge is regarded as a fault current from the inverter's DC connection, as shown in Fig. 7. In contrast to zero governed by state, the capacitor's DC voltage is increased to the required amount depending on the ST duty cycle throughout this mode, not across the load as it would be in zero state operation.

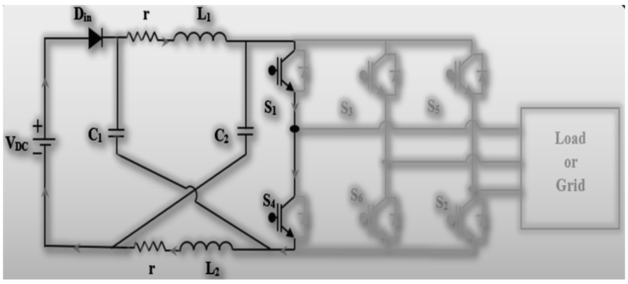

Fig. 7. Equivalent circuit of ZSI viewed from the DC link when the bridge is in a shoot through mode

C) Components design. During in the conventional operating mode, the voltage level is visible across the capacitor but not the inductor since there is no boost involved (only a pure DC current flows through the inductors). The inductor's responsibility is to control the current ripple when Z-source mode (in which boost is used) is active. A linear rise in inductor current occurs during ST, and the voltage across the inductor is much like the voltage across the capacitor. The inductor current drops linearly in non-ST mode (conventional 8 states), as well as the voltage across the inductor seems to be the difference between both the input voltage from the PV and the voltage across the capacitor.

The average current through the inductor is:

$$I_1 = P / P_V, \tag{12}$$

where P is the total power.

Highest ST occurs when there is the greatest current ripple across the inductors. Hence, it is necessary to determine the inductors peak-to-peak current ripple. According to a few applied in diverse studies, it has been discovered that as a general rule, for the majority of ZSI instances, roughly 30 % (or 60 % peak to peak) current ripples is selected for design.

Inductor max current:

$$I_L = I_L + 30\ \%, \tag{13}$$

Inductor min current:

$$I_L = I_L - 30\ \%. \tag{14}$$

Capacitor design. The capacitor reduces current swell and produces a relatively steady voltage that outputs a sinusoidal voltage. According to the mode 3 of Z-source operation and $I_L = I_C$, the capacitor charges the inductor throughout ST. The capacitor values may be roughly determined by limiting the capacitor voltage ripple to about 3 % at peak power, which is often employed in the majority of applications in various publications for ZSI:

$$C = I_l \cdot T_0 / \Delta V_C\ , \tag{15}$$

where in T_0 denotes the switch primary cycle ST time; I_L is the calculated average current either through the inductor:

$$\Delta V_C = V \cdot 3\ \%. \tag{16}$$

Table 1

Operation modes of ZSI

Mode / State	S1	S2	S3	S4	S5	S6
Zero state	ON	OFF	ON	OFF	ON	OFF
	OFF	ON	OFF	ON	OFF	ON
Active state	ON	OFF	ON	OFF	OFF	ON
	OFF	ON	ON	OFF	ON	OFF
	ON	OFF	OFF	ON	ON	OFF
	OFF	ON	OFF	ON	ON	OFF
	ON	OFF	OFF	ON	OFF	ON
	OFF	ON	ON	OFF	OFF	ON
Shoot through state	ON	ON	OFF	OFF	OFF	OFF
	OFF	OFF	ON	ON	OFF	OFF
	OFF	OFF	OFF	OFF	ON	ON

Simulation results and analysis.

A) VSI with SAHF. Using the software MATLAB / Simulink, the PV-SAHF system has been tested. SAHF, which produces compensatory current from reference current retrieved from the mains, is powered by the PV array. Figures 8,*a*,*b*, which depict the PV array's *P-V* and *I-V* characteristics at 25° and 45 °C cell temperatures, respectively and Fig. 8,*c* shows the V_{DC} of VSI. The resulting point on the graph corresponds to the PV array's peak power. At this stage, a P/O MPPT-based controller controls the PV array system for optimal efficiency. The characteristics show that while the open-circuit lowers as the temperature rises, the short-circuit current rises.

The input mains sources current of VSI with the inclusion of a harmonic filter in shunt mode is shown in Fig. 9,*a*. According to Fig. 9,*b*, the PWM-VSI creates the compensatory current to reduce the harmonic currents. Harmonics are cancelled by a compensatory current that has the same amplitude as harmonic components but a 180° phase shift.

Figure 9,*c*, which depicts the source current following SAHF integration, demonstrates how the source current changes to a sinusoidal shape after SAHF integration, becoming harmonic-free. The shunt SAHF system reduces harmonics while enhancing power factor. Figure 9,*c* shows that the source current improves in power factor and is harmonic-free when the SAHF system is connected to VSI .

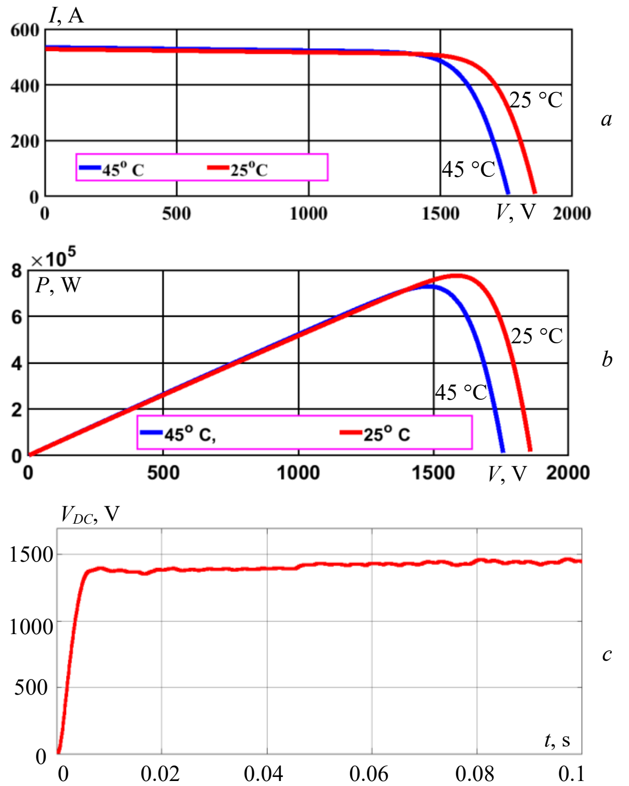

Fig. 8. *a*) *V-I* characteristics of PV array; *b*) *P-V* characteristics of PV array; *c*) V_{DC} of VSI

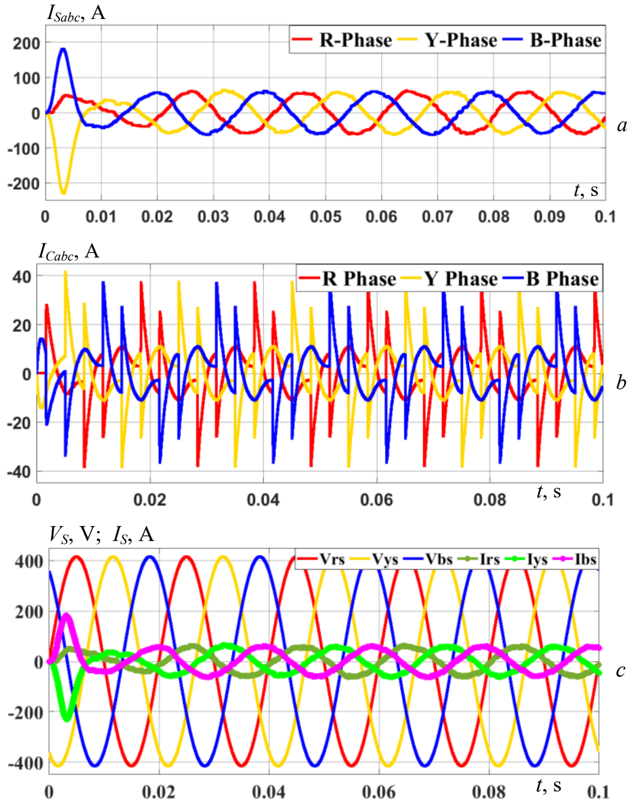

Fig. 9. *a*) Source current at supply mains of VSI with SAHF; *b*) Compensating current of VSI with SAHF; *c*) Power factor improvement of the supply mains by VSI with SAHF

From Fig. 10 shows that the THD is reduced to a satisfactory level when connecting with the SAHF by VSI at fundamental frequency of 50 Hz, THD attained is 7.31 %.

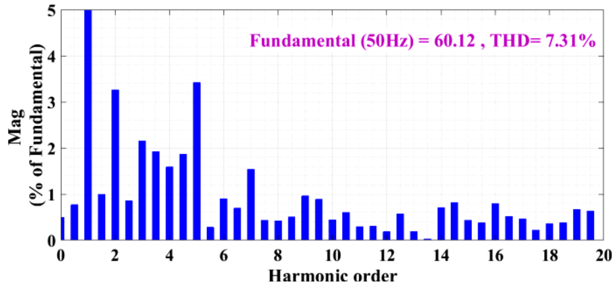

Fig. 10. THD present in source current by VSI with SAHF

B) ZSI with SAHF. MATLAB / Simulink program is being used to test the PV-SAHF system. The SAHF is powered by the PV array, which creates compensatory current using the reference current that was taken from the mains. Figures 11,*a*,*b*, respectively, demonstrate the *P-V* and *I-V* characteristics of the PV array at 25° and 45 °C cell temperature. The resultant graphed point represents the PV array's peak power point. For the PV array system to run as efficiently as possible, a P&O MPPT based controller is used at this stage. The characteristics indicate that when temperature rises, the short-circuit current increases while the open-circuit voltage falls. Figure 11,*c* shows the V_{DC} of the impedance source inverter in accord with all these results.

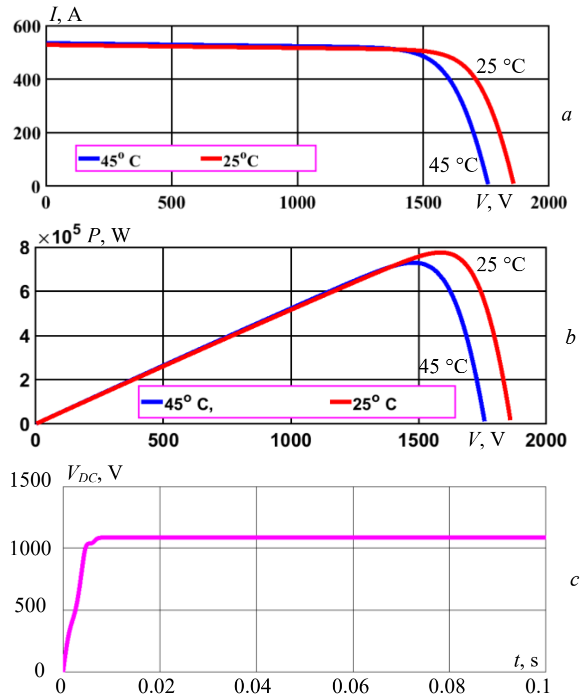

Fig. 11. a) *V-I* characteristics of PV array; *b*) *P-V* characteristics of PV array; *c*) V_{DC} of impedance source inverter

In Fig. 12,*a* the input power supplies source current of the VSI is displayed with the harmonic filter included in the shunt mode. Impedance source inverter produces compensating current to lessen harmonic currents, as seen in Fig. 12,*b*. A compensating current that has a 180° phase shift and the same magnitude as the harmonic components cancels the harmonics. Following SAHF integrations, the source current assumes a sinusoidal form and becomes harmonic-free, as seen in Fig. 12,*c*, which displays the source current during SAHF integration.

The SAHF system reduces harmonics while enhancing power factor. Figure 12,*c* shows that the source current improves in power factor and is harmonic-free when the SAHF system is connected to ZSI.

The SAHF system improves power factor while reducing harmonics. When the SAHF system is linked to ZSI Fig. 12,*c* indicates that the source current has an improved power factor and therefore is harmonic-free.

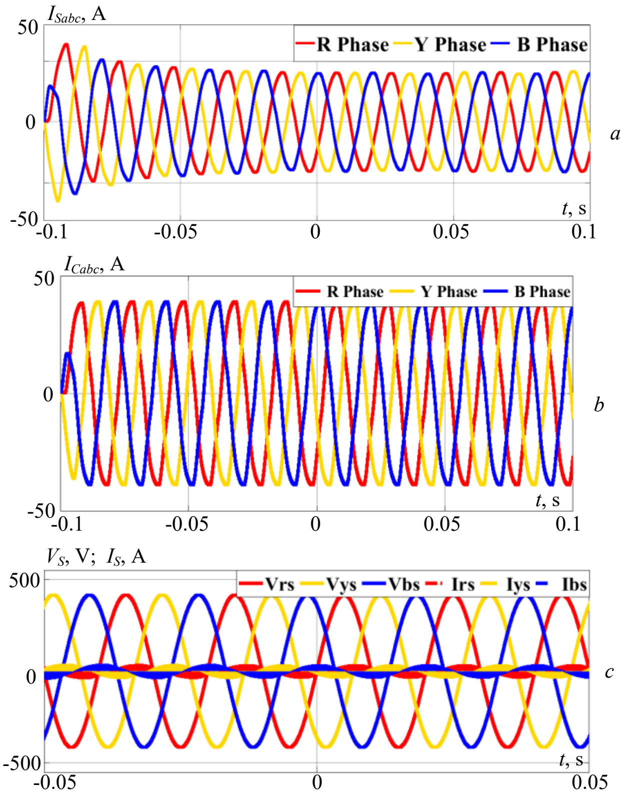

Fig. 12. *a*) Source current at supply mains of ZSI with SAHF; *b*) Compensating current of ZSI with SAHF; *c*) Power factor improvement of the supply mains by ZSI with SAHF

Figure 13 shows that the THD is 1.76 % at 6 kHz when connecting with the SAHF by ZSI at fundamental frequency of 50 Hz.

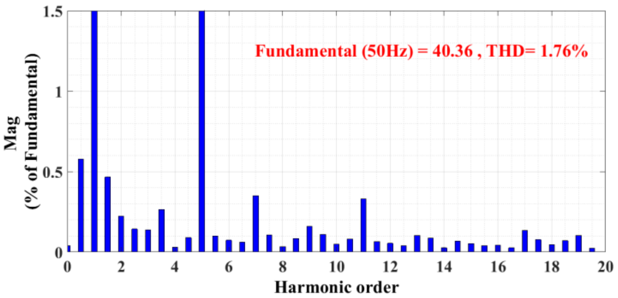

Fig. 13. THD present in source current by ZSI with SAHF

Table 2 shows the comparison between existing topology (VSI with SAHF) and proposed topology (ZSI with SAHF) infers the THD is less in the ZSI.

Table 2

Comparison of SAHF with VSI and ZSI

no.	Topology	Switching frequency, kHz	Parameters				%, THD
			Inductance, mH		Capacitance, mF		
			L_1	L_2	C_1	C_2	
1	VSI with SAHF	5	5	–	0.1	0.012	7.31
2	ZSI with SAHF	5	1.1	1.1	0.5	0.5	1.76

Conclusions.

The primary objectives of the proposed system are to utilize renewable energy sources and include the Z-source inverter architecture. The extra DC-DC converter makes the system more difficult, increases its price, and decreases its effectiveness. Instead of combining DC-DC and DC-AC converters, the suggested system in this setup is a shunt active harmonic filter powered by a photovoltaic source using a Z-source inverter. The use of Z-source inverter helps to overcome the difficulties that conventional topologies are now facing. Analysis of the photovoltaic shunt active harmonic filter system with Z-source inverter performance under various operating conditions in the MATLAB / Simulink environment reveals that the harmonic components are substantially below the stated IEEE norm, which is less than 5 %. Z-source inverter is employed in applications including electric motor drives, photovoltaic power production, and fuel cells because to its special ability to reduce dead time and boost system effectiveness.

Conflict of interest. The authors declare that they have no conflicts of interest.

REFERENCES

1. Manoharan P., Subramaniam U., Babu T.S., Padmanaban S., Holm-Nielsen J.B., Mitolo M., Ravichandran S. Improved Perturb and Observation Maximum Power Point Tracking Technique for Solar Photovoltaic Power Generation Systems. *IEEE Systems Journal*, 2021, vol. 15, no. 2, pp. 3024-3035. doi: https://doi.org/10.1109/JSYST.2020.3003255.

2. Verma N., Jain A., Nishi Ahuja H., Singh G. Maximum Power Point Tracking MPPT Methods for Photovoltaic Modules. *2021 International Conference on Advance Computing and Innovative Technologies in Engineering (ICACITE)*, 2021, pp. 223-227. doi: https://doi.org/10.1109/ICACITE51222.2021.9404571.

3. Shiva C., Bhavani R., Prabha N.R. Power quality improvement in a grid integrated solar PV system. *2017 IEEE International Conference on Intelligent Techniques in Control, Optimization and Signal Processing (INCOS)*, 2017, pp. 1-6. doi: https://doi.org/10.1109/ITCOSP.2017.8303144.

4. Saeed N., Ibrar A., Saeed A. A Review on Industrial Applications of Z-Source Inverter. *Journal of Power and Energy Engineering*, 2017, vol. 05, no. 09, pp. 14-31. doi: https://doi.org/10.4236/jpee.2017.59002.

5. Kumar A., Kumar P. Power Quality Improvement for Grid-connected PV System Based on Distribution Static Compensator with Fuzzy Logic Controller and UVT/ADALINE-based Least Mean Square Controller. *Journal of Modern Power Systems and Clean Energy*, 2021, vol. 9, no. 6, pp. 1289-1299. doi: https://doi.org/10.35833/MPCE.2021.000285.

6. Usha N., Vijaya Kumar M. Power Quality improvement using ZSI based STATCOM in Radial and weakly Meshed Distribution Systems. *International Journal of Advanced Research in Electrical, Electronics and Instrumentation Engineering,* 2013, vol. 2, no. 11, pp. 5365-5372. Available at: https://www.ijareeie.com/upload/2013/november/7_-Power.pdf (Accessed 20.12.2021).

7. Kumar S.K., Ranga J., Pradeep Kumar C.S.K.B., Jayalakshmi S. PV based Shunt Active Power Filter for harmonics mitigation using Decoupled DSRF theory. *2019 5th International Conference on Advanced Computing & Communication Systems (ICACCS)*, 2019, pp. 1108-1110. doi: https://doi.org/10.1109/ICACCS.2019.8728527.

8. Chavan U.M., Thorat A.R., Bhosale S.S. Shunt Active Filter for Harmonic Compensation Using Fuzzy Logic Technique. *2018 International Conference on Current Trends towards Converging Technologies (ICCTCT)*, 2018, pp. 1-6. doi: https://doi.org/10.1109/ICCTCT.2018.8550962.

9. SmitaSinghai S. Compensation of Harmonics of Fully Controlled Loads by Using SAHF. *IOSR Journal of Electrical and Electronics Engineering*, 2017, vol. 12, no. 02, pp. 01-10. doi: https://doi.org/10.9790/1676-1202010110.
10. Sharma K., Shanker S., Gidwani L., Palwalia D.K. An Investigation on Two Stage VSI and ZSI for PV based Single Phase Application. *2019 9th Annual Information Technology, Electromechanical Engineering and Microelectronics Conference (IEMECON)*, 2019, pp. 30-35. doi: https://doi.org/10.1109/IEMECONX.2019.8876978.
11. Teta A., Kouzou A., Rezaoui M.M., Abu-Rub H. Interactive PV-Shunt Active Power Filter based on Impedance Source Inverter Controlled by SRF-MVF. *2021 18th International Multi-Conference on Systems, Signals & Devices (SSD)*, 2021, pp. 306-311. doi: https://doi.org/10.1109/SSD52085.2021.9429460.
12. Rai R., Bhatia R.S., Nijhawan P. DC-DC conversion based on ZSI and boost rectifier using fuzzy logic control. *2016 7th India International Conference on Power Electronics (IICPE)*, 2016, pp. 1-5. doi: https://doi.org/10.1109/IICPE.2016.8079377.
13. Rasul M.J.M.A., Khang H.V., Kolhe M. Harmonic mitigation of a grid-connected photovoltaic system using shunt active filter. *2017 20th International Conference on Electrical Machines and Systems (ICEMS)*, 2017, pp. 1-5. doi: https://doi.org/10.1109/ICEMS.2017.8056401.
14. Jegadeeswari G. Performance analysis of power quality improvement using shunt active power filter. *International Journal of Recent Technology and Engineering*, 2019, vol. 7, no. 5, pp. 1-3. Available at: https://www.ijrte.org/wp-content/uploads/papers/v7i5s2/ES1995017519.pdf (Accessed 20.12.2021).
15. Shaik A.K., Prabhu S., Shaik J., Pathan M.K., Sai M.G. Modelling and Design of Three State Three Switch Buck Boost Inverter. *2020 International Conference on Smart Technologies in Computing, Electrical and Electronics (ICSTCEE)*, 2020, pp. 548-553. doi: https://doi.org/10.1109/ICSTCEE49637.2020.9277431.
16. Saremi Hasari S.A., Soori S., Salemnia A., Khosrogorji S. Z-source DG-active filter. *2016 7th Power Electronics and Drive Systems Technologies Conference (PEDSTC)*, 2016, pp. 248-252. doi: https://doi.org/10.1109/PEDSTC.2016.7556869.
17. Bourouis B., Djeghloud H., Benalla H. Energy efficiency of a 3-level shunt active power filter powered by a fuel-cell / battery DC bus with regulated duty cycles. *Electrical Engineering & Electromechanics*, 2021, no. 5, pp. 30-38. doi: https://doi.org/10.20998/2074-272X.2021.5.05.
18. Baazouzi K., Bensalah A.D., Drid S., Chrifi-Alaoui L. Passivity voltage based control of the boost power converter used in photovoltaic system. *Electrical Engineering & Electromechanics*, 2022, no. 2, pp. 11-17. doi: https://doi.org/10.20998/2074-272X.2022.2.02.

Received 01.06.2022
Accepted 25.07.2022
Published 06.11.2022

B.V. Sai Thrinath[1], *Assistant Professor*, *PhD*,
S. Prabhu[1], *Associate Professor*, *PhD*,
B. Meghya Nayak[2], *Associate Professor*, *PhD*,
[1] Sree Vidyanikethan Engineering College,
Tirupati, AP – 517102, India,
e-mail: connectbvst@gmail.com (Corresponding Author); prabhutajmahal6@gmail.com
[2] Arvind Gavali College of Engineering,
Satara – 415015, Maharashtra, India,
e-mail: meghya29@gmail.com

How to cite this article:
Sai Thrinath B.V., Prabhu S., Meghya Nayak B. Power quality improvement by using photovoltaic based shunt active harmonic filter with Z-source inverter converter. *Electrical Engineering & Electromechanics*, 2022, no. 6, pp. 35-41. doi: https://doi.org/10.20998/2074-272X.2022.6.06